

A Novel Unified Self-alignment Method of SINS Based on FGO

Hanwen Zhou

Harbin Engineering University

Xiufen Ye, Senior Member, IEEE

Harbin Engineering University

The self-alignment process can provide an accurate initial attitude of SINS. The conventional two-procedure method usually includes coarse and fine alignment processes. Coarse alignment converges fast because of its batch estimating characteristics and the initial attitude does not influence the results. But coarse alignment is low accuracy without considering the IMU's bias. The fine alignment is more accurate by applying a recursive Bayesian filter to estimate the IMU's bias, but the attitude converges slowly as the initial value influence the convergence speed of the recursive filter. Researchers have proposed the unified self-alignment to achieve self-alignment in one procedure, existing unified methods make improvements on the basics of recursive Bayesian filter and those methods are still slow to converge. In this paper, a unified method based on batch estimator FGO (factor graph optimization) is raised, which is converge fast like coarse alignment and accurate than the existing method. We redefine the state and rederivation the state dynamic model first. Then, the optimal attitude and the IMU's bias are estimated simultaneously through FGO. The fast convergence and high accuracy of this method are verified by simulation and physical experiments on a rotation SINS.

1

This work was supported in part by State Key Program of the National Natural Science Foundation of China under Grant 41876100; and in part by National Key research and development program of China under Grant 2018YFC0310102.

Hanwen Zhou, Xiufen Ye are with the College of Intelligent System Science and Engineering, Harbin Engineering University, Heilongjiang 150001, China., E-

I. INTRODUCTION

Self-alignment SINS can provide an accurate attitude without additional sensors, and it is widely used in the navigation of unmanned ground vehicles, spacecraft, unmanned surface vehicles and underwater robots.

The conventional two-procedure self-alignment method includes two procedures of coarse alignment and fine alignment. The coarse alignment provides a coarse attitude rapidly. Coarse alignment includes an attitude tracking problem and a constant initial attitude determination problem, where attitude tracking is achieved through attitude update of SINS, the constant initial attitude problem is called Wahba problem, which can be solved by SVD [2]. In recent years, the OBA(optimization-based alignment) has been raised to solve the Wahba problem [1][3][4][5], the methods are still considered as coarse alignment methods because they do not account for the bias error of the IMU.

In two-procedure self-alignment method, fine alignment is employed to refine the results of coarse alignment. Most of the fine alignment methods use a Bayesian filter to estimate the attitude and the bias of IMU, e.g. Kalman filter or PF [6]. In the case of a large initial attitude error, the conventional fine alignment algorithm is easy to diverge and fails to determine the attitude because of the low observability of the heading [8], which explains why coarse alignment is needed before the fine alignment, obtaining a coarse attitude.

Although the two-procedure self-alignment method is now widely used, the sensor data of each procedure can not be shared with the other. It leaves sensor information underutilized, and the waiting time of self-alignment system is longer.

Then researchers tried to find a unified self-alignment algorithm without coarse alignment. Researchers employ the nonlinear error state model with nonlinear Bayesian filter[7][9]. After that, the methods based on Lie group theory were raised to speed up the converge time and improve the converge stability, the Jacobian matrix is independent of the state, e.g. the invariant Kalman filter [15][17] and the state transformation extended Kalman filter [16], while these methods are still based on Bayesian filter, the converge time is still long if the initial heading error is large.

To sum up, the existing unified methods don't combine the fastness of coarse alignment. In order to obtain the advantages of both coarse alignment and fine alignment, a constant initial attitude determined by coarse alignment needs to be added into the fine alignment states. Besides, a batch optimization is necessary.

In recent years, batch estimator FGO are widely used in SLAM and integration navigation [11][12][13][14]. In the application of FGO, the state can be modeled as a constant state and linked to measurements at different times, such as

mail:(yexiufen@hrbeu.edu.cn).(Corresponding author: Xiufen Ye)

the environmental landmarks on SLAM [10], the constant landmark state in SLAM is linked to batch camera image measurements. And this type of factor graph also be called as a graphical state space model [18], which is suitable for estimating the constant initial attitude at the beginning of self-alignment.

There are two main contributions in this paper :

1.Redefine the state and rederivation the state dynamic model.

2.Constructing the self-alignment problem to factor graph, and solving the optimal value through FGO, which is converge fast like coarse alignment and accurate than the existing unified method or two-procedures method.

This paper is structured as follows. The main idea of combining the advantages of the two alignment procedures and the structure of the proposed method are illustrated in section II. The state dynamic model and measurement model of the unified method are given in section III. The unified method based on FGO is proposed in section IV. Simulations and experiments are given in sections V and VI, and the conclusions are summarized in section VII.

II. METHOD OF COMBINING THE COARSE ALIGNMENT WITH FINE ALIGNMENT

In this section, the method of coarse alignment and fine alignment is illustrated, then the advantages and disadvantages of each method are analyzed. After that, the main idea of combining the coarse alignment and fine alignment is discussed. Finally, the system overview of the raised method is given out.

The nomenclature of the frames in this paper is listed in TABLE I, the different coordinates frames can also be seen in Fig. 1.

TABLE I
NOMENCLATURE

| Symbol | Description |
|-------------------|--|
| n | Ideal local level navigation coordinate frame with east-north-up geodetic axes |
| b | Body coordinate frame |
| i_{b_0} | Nonrotating initial body coordinate frame at start time of self-alignment |
| \tilde{i}_{b_0} | The calculated initial body coordinate frame at the start time of self-alignment |
| i_{n_0} | Nonrotating initial navigation coordinate frame at start time of self-alignment |
| i | Nonrotating earth center coordinate frame |
| e | Earth coordinate frame |

As shown in Fig. 1, i is the earth center coordinate frame. i_{b_0} is an inertial frame, which is covered with a body frame at the start time. i_{n_0} is an inertial frame covered with a local navigation frame at the start time. g_n indicates the gravity in n frame.

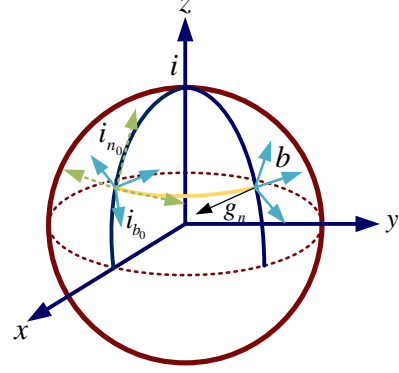


Fig. 1. Coordinate frame definition

A. Coarse alignment

The OBA can divide self-alignment into two parts, one part is the attitude track, which is in charge of solving the DCM (direction cousin matrix) $C_b^{i_{b_0}}$; the other part is in charge of determining the constant initial attitude $C_{i_{b_0}}^{i_{n_0}}$. Since $C_{i_{n_0}}^n = C_n^{i_{n_0}}$ is easy to get, the output DCM C_b^n can be easily given out though $C_b^n = C_n^n C_{i_{b_0}}^{i_{n_0}} C_b^{i_{b_0}}$.

1. Attitude track—calculating the $C_b^{i_{b_0}}$

Differential equation of DCM can be written as (1):

$$\dot{C}_b^{i_{b_0}} = C_b^{i_{b_0}} (\omega_{b_0}^b)^\wedge \quad (1)$$

where, $C_b^{i_{b_0}}$ can be expressed as (2) :

$$C_b^{i_{b_0}} = C_{b_{k-1}}^{i_{b_0}} C_b^{b_{k-1}} \\ C_b^{b_{k-1}} = \exp\left(\left(T\omega_{ib}^i\right)^\wedge\right) \quad (2)$$

Where $\exp(\cdot)$ represents the matrix exponential, $(\cdot)^\wedge$ represents linear, skew-symmetric operator. DCM $C_{b_{k-1}}^{i_{b_0}}$ represent the $C_b^{i_{b_0}}$ before time interval T . this equation can be calculated though Rodriguez formulation [20].

The attitude track doesn't consider the bias error of IMU, the bias error of ω_{ib}^i will lead to a constant growth of the attitude error.

2. Constant initial attitude determination—calculating the $C_{i_{b_0}}^{i_{n_0}}$.

The integration of specific forces in i_{b_0} and the integration of gravity in i_{n_0} can be written as (3) :

$$F_i^{i_{b_0}} = \int_0^{kdt} C_b^{i_{b_0}} f_{sf}^b \\ G_i^{i_{n_0}} = -\int_0^{kdt} g_{i_{n_0}} \quad (3)$$

Where the $C_{i_{n_0}}^{i_{b_0}}$ represents the constant initial attitude, f_{sf}^b is the specific force measurement. $g_{i_{n_0}}$, which is the projection of gravity in i_{n_0} can be expressed as :

$$g_{i_{n_0}} = C_n^{i_{n_0}} g_n$$

$$C_n^{i_{n_0}} = \exp\left(\left(T\omega_{ie}^n\right)^\wedge\right) = \begin{bmatrix} \cos \omega_{ie} t & & & \\ \sin \omega_{ie} t \sin L & & & \\ -\sin \omega_{ie} t \cos L & & & \\ & -\sin \omega_{ie} t \sin L & \sin \omega_{ie} t \cos L & \\ & 1 - (1 - \cos \omega_{ie} t) \sin^2 L & (1 - \cos \omega_{ie} t) \sin L \cos L & \\ & (1 - \cos \omega_{ie} t) \sin L \cos L & 1 - (1 - \cos \omega_{ie} t) \cos^2 L & \end{bmatrix} \quad (4)$$

Where L represents the latitude, $\omega_{ie}^i = [0 \ 0 \ \omega_{ie}]^T$ indicates the rotation rate of the earth and $g_n = [0 \ 0 \ -g]^T$ indicates the gravity vector. Then the relationship between $F_i^{i_{b_0}}$ and $G_i^{i_{n_0}}$ can be expressed as (5).

$$C_{i_{b_0}}^{i_{n_0}} F_i^{i_{b_0}} = G_i^{i_{n_0}} + \int_0^{kdt} C_{i_{b_0}}^{i_{n_0}} \widehat{\nabla}^{b_0} dt$$

$$C_{i_{b_0}}^{i_{n_0}} F_i^{i_{b_0}} \approx G_i^{i_{n_0}} \quad (5)$$

Where $\widehat{\nabla}^{b_0}$ represents the acceleration of disturbance motion, $G_i^{i_{n_0}}$ is the integration of gravity. The DCM form of the Wahba problem can be expressed as (6).

$$C_{i_{b_0}}^{i_{n_0}*} = \min \left(\sum_{k=1}^n \left\| C_{i_{b_0}}^{i_{n_0}} F_i^{i_{b_0}} - G_i^{i_{n_0}} \right\|^2 \right) \quad (6)$$

The optimal $C_{i_{b_0}}^{i_{n_0}}$ can be obtained by solving for this minimum, thus $C_b^n = C_{i_{n_0}}^n C_{i_{b_0}}^{i_{n_0}} C_b^{i_{b_0}}$ can be obtained, and it will not be influenced by initial attitude and can converge rapidly.

B. Fine alignment

The fine alignment models the SINS error as system state x :

$$x = [\phi \ \delta v \ \varepsilon \ \nabla] \quad (7)$$

Where ϕ represents the misalignment angles in the navigation coordinates frame, δv are the velocity errors defined in the navigation frame, ε and ∇ represent the gyro bias errors and accelerometer bias errors respectively. The system state equation and measurement equation can be expressed as (8).

$$\dot{x} = f(x) + W$$

$$z = h(x) + V \quad (8)$$

Then the Bayesian filter, e.g. STEKF or UKF can be employed to estimate the system state. Since these methods are designed with the SINS error model, the final accuracy is higher.

The Bayesian filter is a recursive algorithm, therefore the initial state error has a significant influence on convergence time.

In short, the fine alignment using the Bayesian filter is more accurate, while the convergence of the heading angle is slower.

C. The unified self-alignment method

The conclusions of the coarse alignment and the fine alignment are given in TABLE II.

| Characteristics | Coarse alignment | Fine alignment |
|------------------|------------------|----------------|
| High accuracy | No | Yes |
| Converge rapidly | Yes | No |

The coarse alignment divides the self-alignment into attitude track and constant initial attitude determination. The batch optimization on the constant initial attitude results in faster convergence. The fine alignment contributes to the high accuracy by recursive estimating SINS state including IMU's bias.

Inspired by these ideas, if we design an optimizer that batch solves the optimal value of the misalignment angle and the bias of IMU with the constant initial attitude, the optimizer will have both higher convergence speed and higher accuracy.

The Bayesian filter can not work here because of its recursive nature [19], which resulting in slow convergence at low observability. And the more suitable algorithm is the FGO, which is a batch estimator, the design of the proposed FGO method will be illustrated in section III and section IV.

D. System overview of the unified self-alignment method

The structure of the unified method is shown as Fig. 2, and the procedure of the raised method is given as follows.

1. Calculating the result of attitude track, integration of specific force and gravity, the equation is illustrated in subsection A of section II.

2. Combining the system state determination, the system state model and the measurement model (section III), constructing a factor graph to represent the relationship between measurements and states at different time. Solving the MAP problem of factor graph though minimizing the quadratic sum of factor. This is given in section IV.

3. After we get the optimal misalignment angle and constant initial attitude, the optimal attitude output can be calculated through equation in subsection C of section IV.

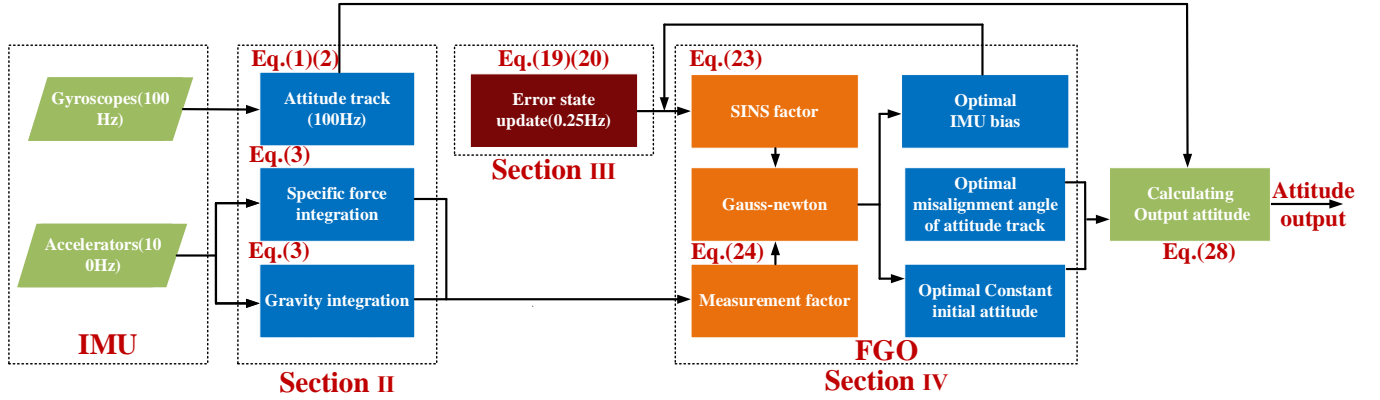


Fig. 2 Structure of this raiste the proposed method

III. SYSTEM STATE MODEL AND MEASUREMENT MODEL

There are two types of nodes in factor graph-variable and factor. Using factor graph, the system state, the system model of state, and the measurement model should be determined first. The system states are structured as variables, and the measurement model and system model are structured as factors.

The regular system model of SINS defined in navigation coordinates frame as shown in (7) can not be used directly, so the dynamic model of SINS defined in i_{b_0} is derived in this section.

A. Redefine the system state

First, we redefine the state that should be estimated in the batch optimizer. The corresponding states of attitude track problem is:

$$x_k = \begin{bmatrix} \phi_k & \delta F_i^{i_{b_0}}(k) & \varepsilon_k & \nabla_k \end{bmatrix} \quad (9)$$

Notice the state is different with state in regular fine alignment (7), and the ϕ_k and $\delta F_i^{i_{b_0}}(k)$ are defined in nonrotating initial body coordinate frame at start time, i_{b_0} , but not in navigation frame. ϕ_k indicates the misalignment angle in i_{b_0} , $\delta F_i^{i_{b_0}}(k)$ represents the error of specific force integration. ε_k represents the gyro's bias error, ∇_k is the accelerator's bias error.

Remarkably, the chosen states of attitude track ϕ_k and $\delta F_i^{i_{b_0}}(k)$ are the error states, this is very important for factor graph expressed by fewer factors. The error state will not change fast, therefore, the state storage interval of the factor graph can be appropriately extended, which reduces the

number of factors and the calculation time.

With the SINS states at different times and the constant initial attitude $C_{i_{b_0}}^{i_{b_0}}$ added into system state, the state of the system can be expressed as (10).

$$X = \begin{pmatrix} x_1 & x_2 & x_3 & \cdots & x_n & C_{i_{b_0}}^{i_{b_0}} \end{pmatrix} \quad (10)$$

The state will be transformed to variables in factor graph.

B. Rederivation the dynamic model of SINS for attitude track

Firstly, the dynamic model of the misalignment angle is derived, and then the dynamic model of the integration of the specific force error is given.

The DCM represents the misalignment angle of SINS, and it can be expressed as:

$$\begin{aligned} C_b^{i_{b_0}} &= C_{i_{b_0}}^{i_{b_0}} \tilde{C}_b^{i_{b_0}} \approx [I + (\phi^\wedge)] C_b^{\tilde{i}_{b_0}} \\ C_b^{\tilde{i}_{b_0}} &\approx [I - (\phi^\wedge)] C_b^{i_{b_0}} \end{aligned} \quad (11)$$

Where $C_b^{\tilde{i}_{b_0}}$ represents the DCM between \tilde{i}_{b_0} and b . Taking the derivation on both sides of the equation (11), the expression is (12).

$$\begin{aligned} \dot{C}_b^{\tilde{i}_{b_0}} &= [-(\dot{\phi}^\wedge)] C_b^{i_{b_0}} + [I - (\phi^\wedge)] C_b^{i_{b_0}} (\omega_{i_{b_0}b}^b)^\wedge = \\ & [-(\dot{\phi}^\wedge)] C_b^{i_{b_0}} + C_b^{\tilde{i}_{b_0}} (\omega_{i_{b_0}b}^b)^\wedge \end{aligned} \quad (12)$$

The differential equation of $C_b^{\tilde{i}_{b_0}}$ can be expressed as:

$$\dot{C}_b^{\tilde{i}_{b_0}} = C_b^{\tilde{i}_{b_0}} \left[\tilde{\omega}_{i_{b_0}b}^b \right] = C_b^{\tilde{i}_{b_0}} \left[\left(\omega_{i_{b_0}b}^b + \delta \omega_{i_{b_0}b}^b \right)^\wedge \right] \quad (13)$$

Where the gyro's rotation rate $\tilde{\omega}_{i_{b_0}b}^b$ is $\tilde{\omega}_{i_{b_0}b}^b = \omega_{i_{b_0}b}^b + \delta \omega_{i_{b_0}b}^b$, $\delta \omega_{i_{b_0}b}^b$ is the measurement error, $\omega_{i_{b_0}b}^b$ represents the ideal rotation rate on b . From equations equation reference goes here and (13), the following equations can be obtained:

$$\begin{aligned}
-(\dot{\phi}^\wedge)C_b^{i_0} + C_b^{i_0}(\omega_{i_0,b}^{b,\wedge}) &= C_b^{i_0} \left[(\omega_{i_0,b}^{b,\wedge} + \delta\omega_{i_0,b}^{b,\wedge})^\wedge \right] \\
-(\dot{\phi}^\wedge) + C_b^{i_0}(\omega_{i_0,b}^{b,\wedge})C_b^{i_0} &= C_b^{i_0}(\omega_{i_0,b}^{b,\wedge})C_b^{i_0} + C_b^{i_0}(\delta\omega_{i_0,b}^{b,\wedge})C_b^{i_0} \\
\dot{\phi}^\wedge &= C_b^{i_0}(\omega_{i_0,b}^{b,\wedge})C_b^{i_0} - C_b^{i_0}(\omega_{i_0,b}^{b,\wedge})C_b^{i_0} - C_b^{i_0}(\delta\omega_{i_0,b}^{b,\wedge})C_b^{i_0} \\
&= -C_b^{i_0}(\delta\omega_{i_0,b}^{b,\wedge})C_b^{i_0} \\
&= -C_b^{i_0}C_b^{i_0}(\delta\omega_{i_0,b}^{b,\wedge})C_b^{i_0} \\
&= -C_b^{i_0}\delta\omega_{i_0,b}^{b,\wedge} \\
&= -[I - (\phi^\wedge)]\delta\omega_{i_0,b}^{b,\wedge} \\
&\approx -\delta\omega_{i_0,b}^{b,\wedge}
\end{aligned} \tag{14}$$

The the attitude error differential equation of SINS is expressed as (15).

$$\dot{\phi}^\wedge = -\delta\omega_{i_0,b}^{i_0} = -C_b^{i_0}\delta\omega_{i_0,b}^b \tag{15}$$

Then we derive the error differential equations of specific force integration.

$$\delta F_i^{b_0} = \tilde{F}_i^{b_0} - F_i^{b_0} \tag{16}$$

Define $\tilde{f}_{sf}^b = f_{sf}^b + \delta f_{sf}^b$ as the specific force measurement in b , where δf_{sf}^b represents the measurement error of specific force. Deriving both sides of (16), the differential equation of error state can be further derived as (17).

$$\begin{aligned}
\delta \dot{F}_i^{b_0} &= C_b^{i_0}\tilde{f}_{sf}^b - C_b^{i_0}f_{sf}^b \\
&\approx C_b^{i_0}(f_{sf}^b + \delta f_{sf}^b) - [I + (\phi^\wedge)]C_b^{i_0}f_{sf}^b \\
&= C_b^{i_0}f_{sf}^b + C_b^{i_0}\delta f_{sf}^b - C_b^{i_0}f_{sf}^b - (\phi^\wedge)C_b^{i_0}f_{sf}^b \\
&= C_b^{i_0}\delta f_{sf}^b - (\phi^\wedge)C_b^{i_0}f_{sf}^b \\
&= C_b^{i_0}\delta f_{sf}^b + (C_b^{i_0}f_{sf}^b)^\wedge \phi
\end{aligned} \tag{17}$$

Since the bias of the IMU does not change in a short time, the dynamic model of SINS can be rewritten as (18).

$$\begin{aligned}
\dot{\phi}^\wedge &= -C_b^{i_0}\varepsilon \\
\delta \dot{F}_i^{i_0} &= C_b^{i_0}\nabla + (C_b^{i_0}f_{sf}^b)^\wedge \phi \\
\dot{\varepsilon} &= 0 \\
\dot{\nabla} &= 0
\end{aligned} \tag{18}$$

And the INS model can be defined as (19).

$$x_{k+1} = f(x_k) + N(0, \Sigma_k^{INS}) \tag{19}$$

Where $f(x_k)$ can be expressed as (20), which is derived by the Eulerian method in the SINS dynamic model (18). And dt is the time interval, which was set to two seconds in the simulations and experiments.

$$f(x_k) = \begin{bmatrix} \phi_k + C_b^{i_0}\varepsilon_k dt \\ \delta F_i^{i_0}(k) + (C_b^{i_0}\nabla_k + (C_b^{i_0}f_{sf}^b)^\wedge \phi_k) dt \\ \varepsilon_k \\ \nabla_k \end{bmatrix} \tag{20}$$

And $N(0, \Sigma_k^{INS})$ indicates the Gauss noise and Σ_k^{INS} is diagonal matrix and represents the noise of the system state.

C. Measurement model of SINS in attitude track

The measurement model can be expressed as (21).

$$z_k = h(x_k, C_{i_0}^{i_0}) + N(0, \Sigma_k^{IOSF}) \tag{21}$$

where $h(x_k, C_{i_0}^{i_0})$ is expressed as:

$$h(x_k, C_{i_0}^{i_0}) = C_{i_0}^{i_0} \int_0^k g^{n_0} dt - (F_i^{i_0}(k) - \delta F_i^{i_0}(k)) \tag{22}$$

And $N(0, \Sigma_k^{IOSF})$ indicates the Gauss noise and Σ_k^{IOSF} is diagonal matrix, representing the noise of integration of specific force.

IV. UNIFIED SELF-ALIGNMENT METHOD OF SINS BASED ON FGO

In section III, the refined SINS model and the measurement model have been illustrated. In this section, we construct a unified self-alignment method based on factor graph optimization.

It is necessary to construct the variables and factors of the factor graph, where the variables correspond to the system states, and the factors correspond to the system state model and the measurement model, which will be given in subsection A.

After that, the MAP problem of factor graph can be exchanged to minimize a quadratic function, which is then solved by a nonlinear optimization algorithm, this will be illustrated in subsection B.

Finally, the equation of optimal attitude output is given in subsection C.

A. Formulations

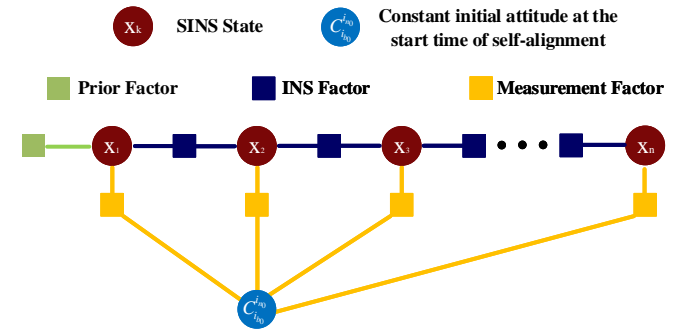


Fig. 3 Factor graph structure of the improved unified self-alignment method in this paper

Fig. 3 shows the factor graph structure of the raised method, in which the variables are represented by circles, set to the system states shown in (10), and the factors are represented by squares, set as follows:

1. INS factor

The error function of INS factor can be expressed as (23).

$$\|e_k^{INS}\|_{\Sigma_k^{INS}}^2 = \|x_{k+1} - f(x_k)\|_{\Sigma_k^{INS}}^2 \quad (23)$$

Where Σ_k^{INS} is diagonal matrix, representing the noise of state prediction.

2.Measurement factor

The error function of measurement factor can be expressed as (24).

$$\|e_k^{IOSF}\|_{\Sigma_k^{IOSF}}^2 = \|z_k - h(x_k)\|_{\Sigma_k^{IOSF}}^2 \quad (24)$$

Where Σ_k^{IOSF} is diagonal matrix, representing the noise of measurement.

3.Prior factor

The error function of Prior factor can be expressed as (25).

$$\begin{aligned} \|e^{PRIOR}\|_{\Sigma^{PRIOR}}^2 &= \|r_{PRIOR} - H_{PRIOR}x_1\|_{\Sigma^{PRIOR}}^2 \\ r_{PRIOR} &= 0_{12 \times 12} \\ H_{PRIOR} &= I_{12 \times 12} \end{aligned} \quad (25)$$

Where Σ^{PRIOR} is diagonal matrix, representing the noise of initial state. With this factor, the self-alignment procedure will be more robust in practice.

B. Optimization and Jacobian calculation

In general, the goal of the multi-sensor integration is to find the optimal posterior state with given sensor measurements. It can be formulated as a typical maximum a posteriori (MAP) problem. The MAP problem can be transformed into finding the variables that maximizes the product of the factors[21]. To get a step further, the X^* can be solved by minimizing a quadratic function[22].

$$X^* = \arg \min \|e_k^{INS}\|_{\Sigma_k^{INS}}^2 + \|e_k^{IOSF}\|_{\Sigma_k^{IOSF}}^2 + \|e^{PRIOR}\|_{\Sigma^{PRIOR}}^2 \quad (26)$$

Then the Gauss-Newton optimization or the Levenberg-Marquardt method is employed to minimize this function. Using the Gauss-Newton algorithm needs to calculate the Jacobian matrix, however, the Jacobian of the DCM is special and can not be calculated directly. The perturbation φ is applied on the left respect to DCM [20], then the Jacobian matrix can be calculated as (27).

$$\begin{aligned} \frac{\partial h(x_k, C_{i_{b_0}}^{i_{b_0}})}{\partial C_{i_{b_0}}^{i_{b_0}}} &= \lim_{\varphi \rightarrow 0} \frac{\exp(\varphi^\wedge) \exp(\xi^\wedge) \int_0^k g^{n_0} dt - \exp(\xi^\wedge) \int_0^k g^{n_0} dt}{\varphi} \\ &\approx \lim_{\varphi \rightarrow 0} \frac{(I + \varphi^\wedge) \exp(\xi^\wedge) \int_0^k g^{n_0} dt - \exp(\xi^\wedge) \int_0^k g^{n_0} dt}{\varphi} \\ &= \lim_{\varphi \rightarrow 0} \frac{(\varphi^\wedge) \exp(\xi^\wedge) \int_0^k g^{n_0} dt}{\varphi} \\ &= \lim_{\varphi \rightarrow 0} \frac{-\left(\exp(\xi^\wedge) \int_0^k g^{n_0} dt\right)^\wedge}{\varphi} \\ &= -\left(C_{i_{b_0}}^{i_{b_0}} \int_0^k g^{n_0} dt\right)^\wedge \end{aligned} \quad (27)$$

C. Optimal attitude output

After getting the optimal $C_{i_{b_0}}^{i_{b_0}}$ and $C_{i_{b_0}}^{i_{b_0}}$, the optimization output DCM can be expressed as (28).

$$C_b^n = C_{i_{a_0}}^n C_{i_{b_0}}^{i_{a_0}} C_{i_{b_0}}^{i_{b_0}} C_b^{i_{b_0}} \quad (28)$$

V. SIMULATION

A. SIMULATIONS SETUP

The simulation compared the heading results of four different methods, the first is the conventional two procedure method OBA with Kalman filter[6], in which the coarse alignment method works for the first 120s, followed by Kalman filtering; the second is the unified method ST-EKF [16], the third is the OBA method to estimate the initial attitude [4] and the last one is the method raised in this paper.

Simulation tests were set up under mooring conditions, adding bias error to raw data, where $\varepsilon_x^b = -8^\circ/h$, $\varepsilon_y^b = 6^\circ/h$, $\varepsilon_z^b = -7^\circ/h$, $\nabla_x^b = 1mg$, $\nabla_y^b = -1mg$, $\nabla_z^b = 1mg$. And the IMU was continuously rotated [23] to improve the observability of the misalignment angle and bias of gyros. The SINS devices accuracy and rotation pattern were consistent with the physical experiment conditions in section VI.

Each method had been tested for 15 minutes, and RMSE (Root Mean Square Error) was chosen as the evaluation criterion.

B. SIMULATION RESULTS AND ANALYSIS

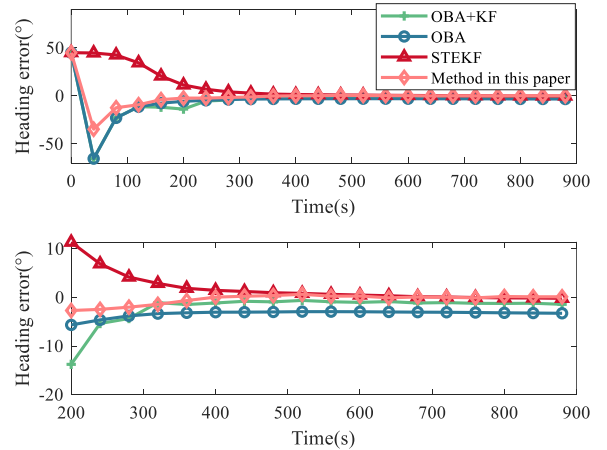


Fig. 4 Heading error of different methods

As shown in Fig. 4, the top half of the figure is the heading error among 900 seconds. Initially, the heading errors of the STEKF and KF with recursive characteristics converge slower. Owing to all the sensor data recorded, our raised method and the OBA method find the optimal initial attitude directly, and the initial heading error will not affect the FGO.

TABLE III
HEADING RMSE OF DIFFERENT SELF-ALIGNMENT METHODS

| Average heading RMSE | OBA+KF | OBA | STEFK | our method |
|----------------------|--------|-------|-------|--------------|
| 200-250 sec | 8.868 | 4.882 | 8.466 | 2.364 |
| 300-350 sec | 1.962 | 3.375 | 2.726 | 1.189 |
| 850-900 sec | 1.380 | 3.259 | 0.175 | 0.107 |

Then the heading RMSE comparison in different times is shown in TABLE III.

Between 200 to 250 seconds, the RMSE of the OBA method and the raised method outperform STEKF and KF, because batch estimation converges faster than the Bayesian filter during self-alignment.

Between 300 to 350 seconds, the heading RMSE of the raised method is 1.189, and it's performance is still the best. The heading RMSE of KF STEKF and the proposed method is smaller than OBA, because they estimate the gyro's bias. As shown in Fig. 5, all three methods estimate the bias of the gyro x-axis and the y-axis successfully.

Between 850 to 900 seconds, the STEKF starts to have the same RMSE with the raised method.

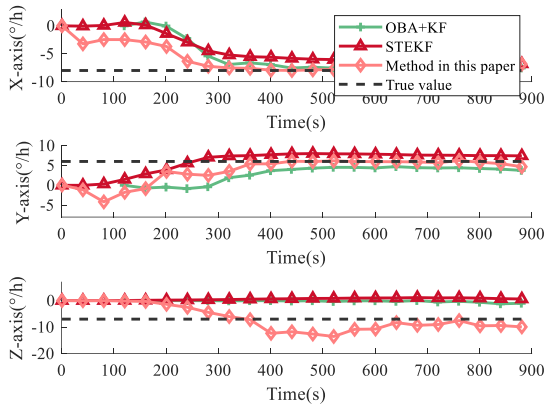


Fig. 5 Estimated results of Gyro bias

From the simulation results, it can be seen that the raised method has better performance than other methods with the same alignment time. There are two reasons why the raised method has a better accuracy:

1. The main reason is the batch estimator converges more rapidly than the recursive Bayesian filter in self-alignment.
2. In each iteration of FGO, a re-linearization is performed, and multiple re-linearizations can effectively mitigate the linearization error.

To sum up, there are two conclusions.

1. At the beginning, the raised method has a rapid initial converge speed as the coarse alignment method OBA. And this is better than STEKF with a large initial heading misalignment angle.

2. With the same alignment time, the raised method is more accurate than KF and STEKF with the rapid converge speed and the multiple re-linearization.

VI. PHYSICAL EXPERIMENT

A. PHYSICAL EXPERIMENT SETUP

Dual-antenna receivers were set as attitude references. As shown in Fig. 6, GPS antennas were set up in the fore and aft of a ship, and the length of the baseline was 15 meters. Thus, the accuracy of the attitude reference was about $0.2^\circ / 15 \approx 0.013^\circ$. The system was fixed on the deck of the ship. All of the connections were tight.

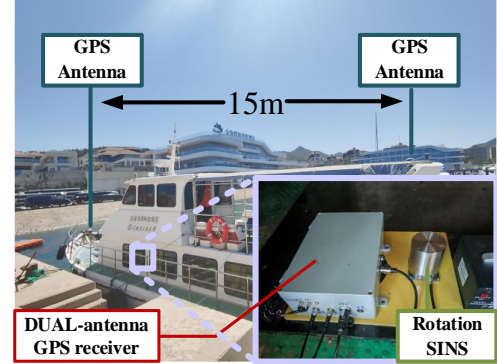


Fig. 6. Experiment ship and experiment system

The performance of the experiment rotation SINS is shown in TABLE IV.

TABLE IV
PERFORMANCE OF THE ROTATIONAL SINS

| Parameters | Value |
|--------------------------------|---------|
| Gyro bias repeatability | 2.00°/h |
| Gyro bias stability | 0.1°/h |
| Gyro random walk | 0.1°/√h |
| Gyro scale factor accuracy | 100ppm |
| Accelerator bias repeatability | 20.0ug |

The self-alignment experiments were carried out 5 times, 15 minutes each time, and RMSE was selected as the evaluation criteria.

B. EXPERIMENT RESULTS

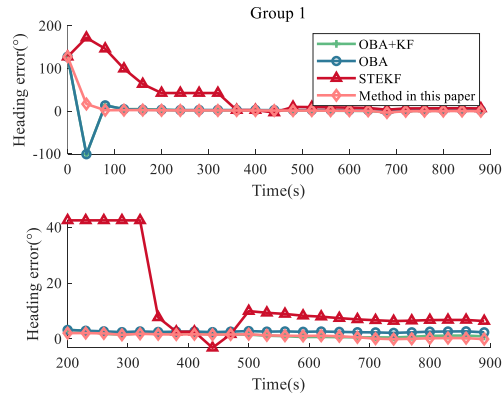


Fig. 7 Heading error comparison of group 1

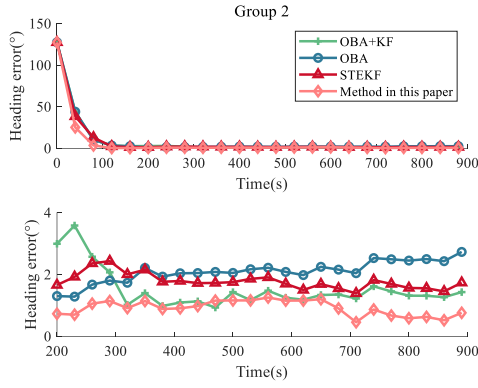


Fig. 8 Heading error comparison of group 2

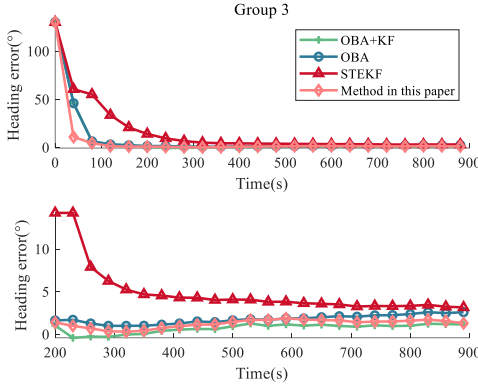


Fig. 9 Heading error comparison of group 3

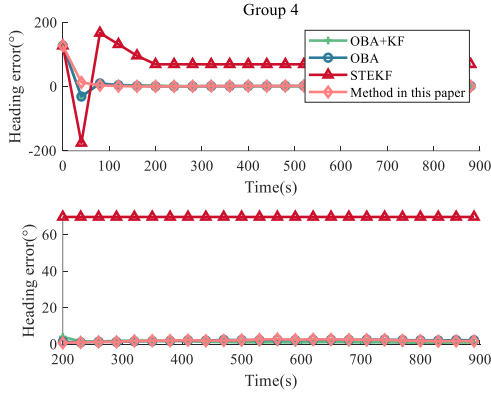


Fig. 10 Heading error comparison of group 4

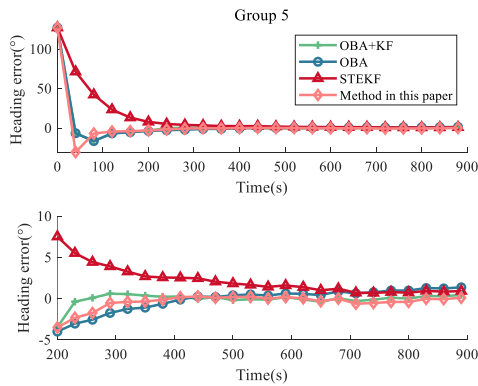


Fig. 11 Heading error comparison of group 5

The top half of Fig. 7 to Fig. 11 is the heading error among 900 seconds, and the bottom half of the figures is the heading error among 200 to 900 seconds.

From these figures, it can be seen that the OBA method and the raised method converged rapidly, and the detailed comparison on the average RMSE of the five groups is given in TABLE V.

TABLE V
HEADING RMSE OF DIFFERENT SELF-ALIGNMENT METHODS

| Average heading RMSE(°) | OBA +KF | OBA | STEKF | Method in this paper |
|-------------------------|---------|-------|---------------------|----------------------|
| 200-250 sec | 2.382 | 2.063 | 7.042 | 1.530 |
| 300-350 sec | 1.155 | 1.660 | 1.127 | 1.054 |
| 850-900 sec | 1.091 | 2.310 | 2.035 (group 2 3 5) | 0.952 |

The STEKF performed badly in experiment group 1 and group 4, because the initial heading misalignment angle is too large that the STEKF cannot converge in the limit time, so the these two groups' date of STEKF will not be calculated in average value.

Between 200 to 250 seconds, the accuracy of the OBA method and the raised method are better than STEKF and KF, because the batch estimation converges faster than the Bayesian filter during self-alignment.

Between 300 to 900 seconds, the heading RMSE of KF STEKF and the raised method are less than OBA's, because they estimate the gyro's bias.

With the same alignment time, the raised method has lower RMSE, although the RMSE differences between different methods decrease over time.

To sum up, there are two conclusions.

1. At the beginning, the raised method has a rapid initial converge speed as OBA of coarse alignment. Which is better than STEKF with a large initial heading misalignment angle.

2. With the same alignment time, the raised method is more accurate than KF and STEKF with the rapid converge speed and the multiple re-linearization.

VII. CONCLUSIONS

This paper raised a novel unified self-alignment method of SINS based on FGO. Firstly, the system model of SINS in initial body coordinates frame is deduced. Then the estimation problem of factor graph is constructed. Finally, the initial constant attitude, the misalignment angle of attitude tracking, and the bias are estimated through FGO.

Combining batch estimation of the SINS state and the constant initial attitude, the unified method successfully combines the advantage of coarse alignment and fine alignment. There are two conclusions in this paper.

At the beginning time of self-alignment, the raised method based on batch estimator converges more rapidly than those method using the Bayesian filter.

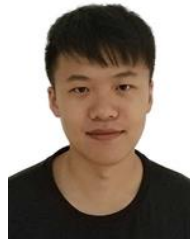
With the same self-alignment time, the raised method is more accurate than KF and STEKF with the rapid converge speed and the multiple re-linearization.

Hence, with the raised method, a higher accuracy can be

achieved in a shorter time.

REFERENCES

- [1] P. M. G. Silson, "Coarse Alignment of a Ship's Strapdown Inertial Attitude Reference System Using Velocity Loci," *IEEE Transactions on Instrumentation and Measurement*, vol. 60, no. 6, pp. 1930-1941, 2011.
- [2] G. Wahba, "A least squares estimate of satellite attitude," *SIAM Rev.*, vol. 7, no. 3, p. 409, 1965.
- [3] L. B. Chang, J. S. Li and K. L. Li, "Optimization-based Alignment for Strapdown Inertial Navigation System: Comparison and Extension," *IEEE Transactions on Aerospace and Electronic Systems*, vol.52, no. 4, pp. 1697-1713, 2016
- [4] Y. Wu, X. Pan, Velocity/Position Integration Formula Part I: Application to In-flight Coarse Alignment, *IEEE Trans. Aerosp. Electron. Syst.*, vol. 49, no. 2, pp. 1006–1023, Apr. 2013.
- [5] J. Li, W. Gao, Y. Zhang and Z. Wang, "Gradient Descent Optimization-Based Self-Alignment Method for Stationary SINS," in *IEEE Transactions on Instrumentation and Measurement*, vol. 68, no. 9, pp. 3278-3286, Sept. 2019, doi: 10.1109/TIM.2018.2878071.
- [6] J. C. Fang, and D. J. Wan, "A fast initial alignment method for strapdown inertial navigation system on stationary base," *IEEE Transactions on Aerospace and Electronic Systems*, vol. 32, no. 4, pp.1501-1505, 1996.
- [7] H. J. Shao, L. J. Miao, W. X. Gao and J. Shen, "Ensemble Particle Filter Based on KLD and Its Application to Initial Alignment of the SINS in Large Misalignment Angles," *IEEE Transactions on Industrial Electronics*, vol. 65, no. 11, pp. 8946-8955, 2018.
- [8] F.O. Silva, E.M. Hemery and W. C. L. Filho, "On the measurement selection for stationary SINS alignment Kalman filters," *Measurement*, vol. 130, pp.82-93, 2018.
- [9] H. S. Hong, J. G. Lee and C. G. Park, "Performance improvement of in-flight alignment for autonomous vehicle under large initial heading error," *IEE Proc.-Radar Sonar Navigation*, vol. 151, pp. 57-62, 2004.
- [10] T. Qin, P. Li and S. Shen, "VINS-Mono: A Robust and Versatile Monocular Visual-Inertial State Estimator," in *IEEE Transactions on Robotics*, vol. 34, no. 4, pp. 1004-1020, Aug. 2018, doi: 10.1109/TRO.2018.2853729.
- [11] Wen, W. , et al. "It is time for Factor Graph Optimization for GNSS/INS Integration: Comparison between FGO and EKF." (2020).
- [12] Tang, H. , et al. "Exploring the Accuracy Potential of IMU Preintegration in Factor Graph Optimization." (2021).
- [13] W. Ding, S. Hou, H. Gao, G. Wan and S. Song, "LiDAR Inertial Odometry Aided Robust LiDAR Localization System in Changing City Scenes," 2020 IEEE International Conference on Robotics and Automation (ICRA), 2020, pp. 4322-4328, doi: 10.1109/ICRA40945.2020.9196698.
- [14] V. Indelman, S. Williams, M. Kaess and F. Dellaert, "Factor graph based incremental smoothing in inertial navigation systems," 2012 15th International Conference on Information Fusion, 2012, pp. 2154-2161.
- [15] A. Barrau and S. Bonnabel, "The Invariant Extended Kalman Filter as a Stable Observer," in *IEEE Transactions on Automatic Control*, vol. 62, no. 4, pp. 1797-1812, April 2017, doi: 10.1109/TAC.2016.2594085.
- [16] M. Wang, W. Wu, X. He and X. Pan, "State Transformation Extended Kalman Filter for SINS based Integrated Navigation System," 2019 DGON Inertial Sensors and Systems (ISS), 2019, pp. 1-14, doi: 10.1109/ISS46986.2019.8943781.
- [17] Chang, L. , Qin, F. , & Xu, J. . (2021). Strapdown inertial navigation system initial alignment based on group of double direct spatial isometries.
- [18] S. Lü, "Graphical State Space Model," 2021 IEEE International Conference on Unmanned Systems (ICUS), 2021, pp. 637-643, doi: 10.1109/ICUS52573.2021.9641466.
- [19] Thrun, & Sebastian. (2005). Probabilistic robotics. Communications of the Acm, 45(3), 52-57.
- [20] Barfoot, T. D. . "State estimation for robotics." (2017)..
- [21] M. Kaess, A. Ranganathan and F. Dellaert, "iSAM: Incremental Smoothing and Mapping," in *IEEE Transactions on Robotics*, vol. 24, no. 6, pp. 1365-1378, Dec. 2008, doi: 10.1109/TRO.2008.2006706.
- [22] Frank Dellaert; Michael Kaess, Factor Graphs for Robot Perception , now, 2017.
- [23] B. Liu, S. Wei, J. Lu, J. Wang and G. Su, "Fast Self-Alignment Technology for Hybrid Inertial Navigation Systems Based on a New Two-Position Analytic Method," in *IEEE Transactions on Industrial Electronics*, vol. 67, no. 4, pp. 3226-3235, April 2020, doi: 10.1109/TIE.2019.2910045.



Hanwen Zhou was born in 1995. He received the B.S. degree in Measurement and Control Technology and Instrumentation, and received the M.S. degree in Control Science and Engineering from Harbin Engineering University, Harbin, China in 2017 and 2020. He is currently pursuing the Ph.D. degree in control science and engineering

with the School of College of Intelligent System Science and Engineering, Harbin Engineering University, China. His current research interests include underwater navigation and intelligent control of underwater automatic vehicles.



Xiufen Ye (Senior Member, IEEE) was born in 1966. She received the B.S., M.S., and Ph.D. degrees in control theory and control engineering from Harbin Shipbuilding Engineering University (Harbin Engineering University), Harbin, China, in 1987, 1990, and 2003, respectively. She has been a Professor with

the College of Automation, Harbin Engineering University, since September 2003. She is the author of more than 200 articles. She holds more than 20 patents. Her current research interests include underwater vehicle intelligent control systems, digital image processing, and object detection and tracking. She was a recipient of the two provincial and ministerial science and technology progress awards. She has served as the Program Committee Chair for the IEEE ICIA 2010 and the IEEE/ICME CME 2011.